THE GEOLOGICAL SOCIETY OF AMERICA®

Tectonic regime controls clustering of deformation bands in porous sandstone

Roger Soliva[1], Gregory Ballas[2], Haakon Fossen[3], and Sven Philit[1]
[1]Geosciences Montpellier, Université de Montpellier, Campus Triolet, CC060, Place Eugène Bataillon, 34095 Montpellier Cedex 05, France
[2]Institut Français de Recherche pour l'Exploitation de la Mer, Pointe du Diable, 29280 Plouzané, France
[3]Department of Earth Science and Museum of Natural History, University of Bergen, Allégaten 41, N-5007 Bergen, Norway

ABSTRACT

Porous sandstones tend to deform by the formation of low-permeability deformation bands that influence fluid flow in reservoir settings. The bands may be distributed or localized into clusters, and limited recent data suggest that tectonic regime may exert control on their distribution and clustering. In order to explore this suggestion, we performed a synthetic analysis based of 73 sets of bands, including 22 new sets measured for a reverse Andersonian regime that fill the important gap in data for this context. We find a surprisingly strong correlation between clustering and tectonic regime, where bands clearly are more distributed in the reverse regime compared to the normal regime. Together with the observed band distributions, capillary pressure data show evidence that efficient membrane seals are expected for extension, whereas pervasive permeability anisotropy is expected for contraction. Such a basic new rule concerning tectonic regime is very useful for assessment of reservoir properties where deformation bands are common but below seismic resolution.

INTRODUCTION

Tectonic deformation in porous sandstones generally produces cataclastic deformation bands in which grain crushing, sliding, and rolling take place (Aydin, 1978; Fossen et al., 2007). The result is typically grain-size reduction that causes porosity loss and reduction of permeability by up to six orders of magnitude (Fossen and Bale, 2007; Ballas et al., 2015). Different classes of cataclastic deformation bands have been recognized as a function of their relative amount of shear to compaction, including shear bands (SBs), compactional shear bands (CSBs), shear-enhanced compaction bands (SECBs), and pure compaction bands (PCBs) (Eichhubl et al., 2010; Soliva et al., 2013). Some of their properties, such as displacement-length scaling relationships (Schultz et al., 2008), degree of cataclasis, petrophysical properties (Ballas et al., 2014), and spatial distribution (Fortin et al., 2005; Saillet and Wibberley, 2010), seem directly linked to such differences in kinematics. Identifying the internal and external factors controlling such differences in band kinematics could be of primary importance for sandstone reservoir characterization.

Both mechanical tests and field data in porous sandstones suggest that many factors, including grain size, porosity, proximity to faults, segmentation, burial depth, and potentially fluid pressure, are thought to influence the spatial distribution of deformation bands and their relative amount of shear to compaction (e.g., Wibberley et al., 2007; Solum et al., 2010; Nicol et al., 2013; Soliva et al., 2013; Ballas et al., 2014). In this paper we inspect the role of tectonic regime on the spatial distribution of deformation bands with new data collected from 22 outcrops in contractional settings in California and Nevada (USA), France, Germany, and Taiwan. This allows for a sound synthetic analysis of band distribution in reverse regimes compared to data in normal regimes collected from the literature. We briefly discuss the origin of the observed general trend and implications for sandstone reservoirs.

GEOLOGIC SETTINGS

Band frequency data (number of bands per meter) were measured in Nevada in the fine- to medium-grained porous Jurassic Aztec Sandstone (Fossen et al., 2015). This unit was involved in the Cretaceous Sevier orogeny with the east to southeast transport of the Muddy Mountain thrust sheet. Data were collected from three principal sites: one in the Buffington window and two in the Valley of Fire State Park.

In California, data were collected from oil-filled porous sandstones of the Edna Member of the Miocene–Pliocene Pismo Basin (Antonellini et al., 1999). This basin occupies a syncline limited by the Edna thrust fault to the northeast. Layers containing deformation bands show a wide range in grain size (fine-grained sand to gravel). Measurements were made on one outcrop but are separated into three sets because of the different band distributions observed in the different layers.

In France, we measured band sets in the porous Cretaceous sandstones of the South East Basin (Ballas et al., 2014). These marine sandstones were folded and faulted during the north-south Paleocene–Eocene Pyrenean shortening, and data from ten outcrops are reported here for host rocks showing medium to coarse grain sizes.

Data from Germany were collected from the Alpine Subhercynian Basin in the medium-size porous sandstones of the lower Cretaceous Involutus and Heidelberg formations (Klimczak and Schultz, 2013). This basin is folded and mainly faulted at its southwestern border by the Harz Mountains thrust. Data reported in this paper are from four outcrops observed at different places in the basin; one outcrop is very close to the Harz thrust, and three others are relatively far from the thrust (>2 km).

Cataclastic bands from Taiwan are located on the east coast (Shihtiping), in fine- to coarse-grained volcanic-tuff sandstones. These deposits are related to the formation of the Coastal Range due to the arc-continent collision ~7 m.y. ago. A north-south–striking fold affects these deposits, and two band sets were measured in the site.

BAND SET GEOMETRY, FREQUENCY, AND CLUSTERING

Methods

Because many workers have counted the number of individual bands per meter, we proceed in the same way, using a tape ruler along outcrops, to allow for a global data synthesis. Most data sets from the Andersonian normal stress regime were acquired along scan lines oriented along the direction of maximum extension (X axis of the strain ellipsoid). For the new measurements provided for the Andersonian reverse stress regime, we counted the bands along a scan line oriented along the direction of maximum shortening (Z axis).

Band Set Geometry

Outside of fault zones, cataclastic deformation bands forming reverse band sets are generally pervasive sets of SECBs or CSBs. SECBs generally

show no visible displacement in the field and crop out as conjugate sets that intersect only in some parts of the outcrops (Fig. 1A). CSBs generally crop out as regular mesh-like geometries of conjugate crosscutting bands (Fig. 1B), along which reverse-sense displacement of a few centimeters can be observed. Both types of band sets are very rare in fine sandstones, and are generally restricted to specific layers of medium to coarse porous sandstone. Within the deformed layers, the spatial distribution of the bands is extensive, generally over entire outcrop exposures (tens of meters to 100 m) with more or less evenly spaced bands (Figs. 1A and 1B). Note, however, that SBs organized as clusters can also be observed in reverse regime, but specifically located within fault zones (see Fig. 1E, Subhercynian).

Bands in the normal regime are typically CSBs and SBs clustered around normal faults, defining damage zones. Damage zones are characterized by a steep increase in band density toward a main fault surface,

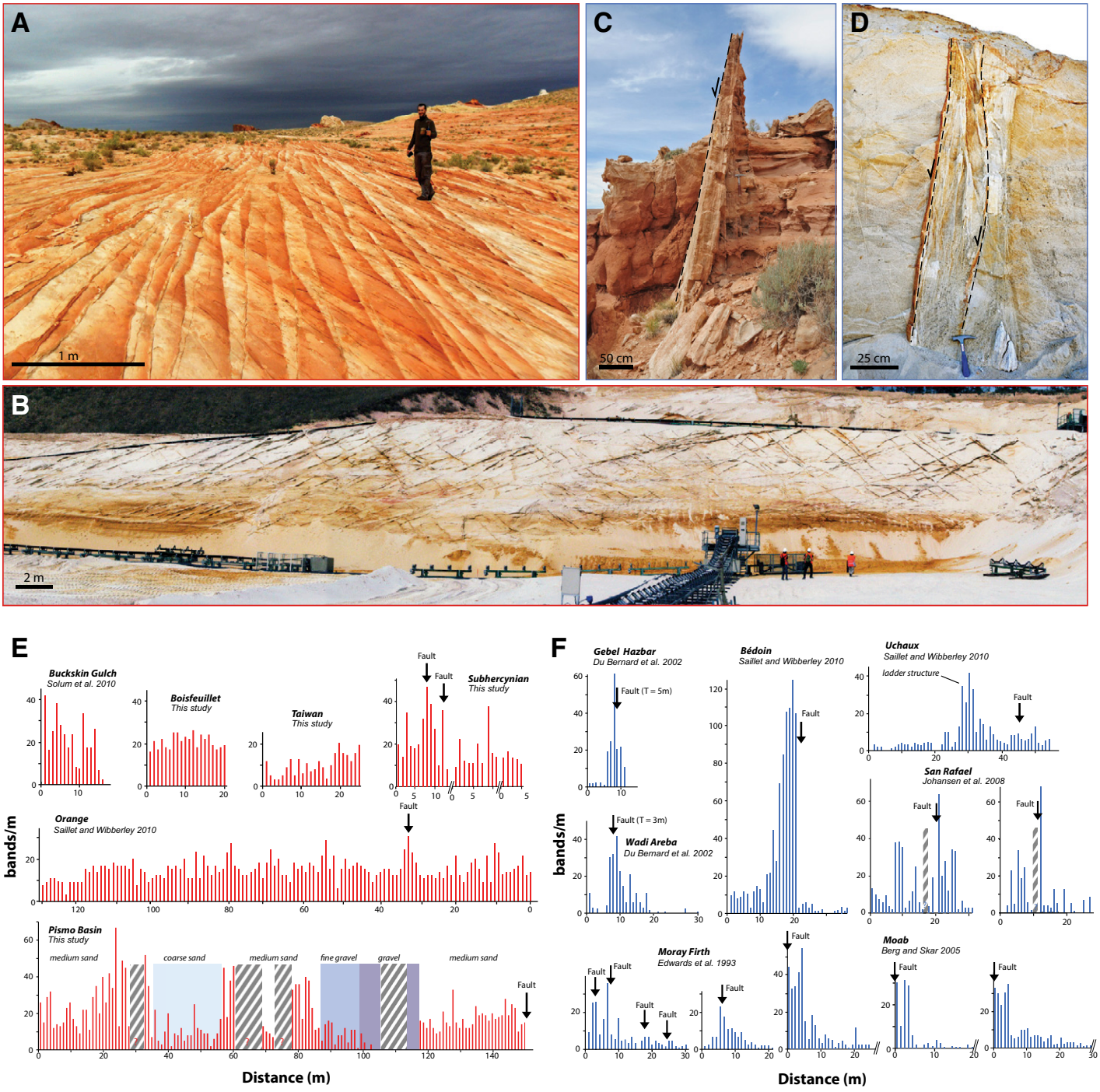

Figure 1. Examples of geometry and spatial distribution of band sets formed as reverse and normal Andersonian regimes. A: Reverse set of shear-enhanced compaction bands in Valley of Fire Sate Park (Nevada, USA) seen as limiting red oxidations. B: Reverse set of compactional shear bands in the Les Crans quarry (Provence, France). C: Normal shear band cluster adjacent to normal fault surface near Goblin Valley State Park (Utah, USA). D: Normal shear band cluster at the vicinity of two fault surfaces in the Boncavaï quarry (Provence, France). E: Histograms of number of band per meter versus distance along scan lines for various reverse band sets. F: Same type of histograms as shown in E, for normal band sets. Zones striped in gray mark intervals where the sandstone is not exposed. See Data Repository (see footnote 1) for references cited in E and F.

which is located along or within a central cluster zone (Figs. 1C and 1D). In addition, clusters can also occur as incipient fault structures far from established fault surfaces. SBs in the clusters are spaced a few millimeters or centimeters apart, and generally oriented subparallel to the fault. Bands can form parallel or conjugate sets, as branching or mutually crosscutting structures. These SBs can show centimeter- to decimeter-scale displacements and generally display more intense cataclasis than CSBs and SECBs.

Histograms of number of bands per meter are shown in Figure 1E for some of the most representative reverse band sets. These graphs show nearly homogeneous to polymodal distribution with some modes that are located at places where few faults or ladder structures are observed (see Schultz and Balasko, 2003, for definition of ladder structure). For all the reverse band sets reported in the literature (see Figure 2, and the GSA Data Repository[1] for references), the mean value of bands per meter is 12, with a standard deviation of 9.6. The spatial distribution is particularly heterogeneous in outcrops showing variations in lithology, such as in the Pismo Basin (Fig. 1E). Relatively high values of bands per meter are observed in medium-grained units (generally >10 bands/m), while lower band frequencies are observed in coarse-grained units (generally <10 bands/m), and few bands are observed in the sand matrix of gravel units. Fine sandstones, cemented sandstones, or other low-porosity rock layers are devoid of SECBs or CSBs.

The distribution of normal sense bands per meter appears Gaussian or log-normal; see Figure 1F for some of the most representative normal band sets measured. These modal distributions generally show a progressive increase in band density to a maximum value (cluster), into which bands are very closely packed (Fig. 1C). An asymmetric distribution (log-normal distribution type) generally reflects the juxtaposition of differently damaged units around a fault surface. For all the normal band sets collected from the literature (Fig. 2), the maximum number of bands per meter reaches the value of 161. Also note that zones devoid of bands are shown on the graphs presented in Figure 1F.

Data Synthesis Analysis

We synthesized all the band density data obtained from our field work and from the literature; 24, 47, and 2 band sets from the reverse, normal, and strike-slip regimes, respectively. These 73 sets represent a total of 27,074 bands recorded along scan lines from sandstones showing a wide range in porosity (18.6%–35.14%), grain size (0.24 mm in diameter to gravel sized), burial depth (0.3–2.5 km), and diagenetic context.

To precisely examine the relative spatial distribution of bands of all sets together, we calculate the cluster factor (Wibberley et al., 2007) for each set. This parameter is a standard deviation–type function describing the degree of clustering within a given band set along a scan line. The cluster factor is defined as:

$$Cf = \sqrt{\frac{\sum f_i^2}{\sum f_i} - f_{av}}, \quad (1)$$

where f_i is the number of bands encountered per meter of scan line, i represents the i^{th} meter interval along the scan line, and f_{av} is the average band frequency for the entire scan line. For all the band sets collected and measured, this factor varies between 0.47 and 8.78, where 8.78 corresponds to the highest band clustering and 0.47 is the most even band distribution.

A global data analysis shows a clear difference between reverse and normal band sets with respect to spatial distribution. Figure 2 presents all band sets measured by us and collected from the literature as a function of the cluster factor and the maximum value of bands per meter. This graph

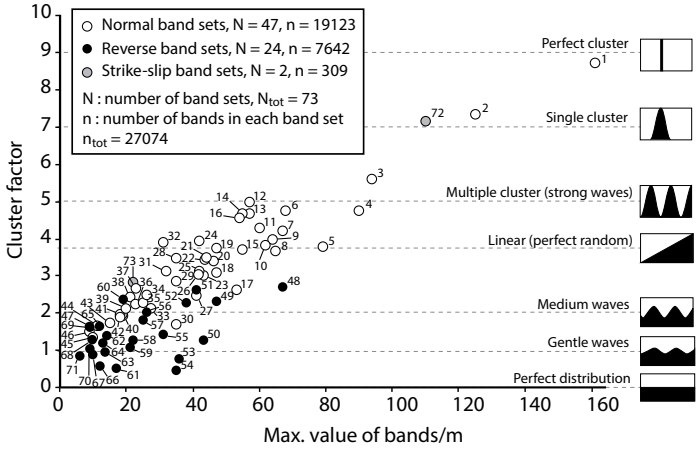

Figure 2. Data set synthesis of reverse (black circles), normal (white circles), and strike-slip (gray circles) band sets plotted as cluster factor versus maximum value of bands per meter. Schemes of synthetic data distribution are shown for different values of cluster factor. Band sets are numbered. For numbered references and number of bands per set, see the Data Repository (see footnote 1).

reveals that reverse band sets (black circles) have a low cluster factor, but also low values of maximum bands per meter as compared to normal band sets. Reverse band sets have cluster factor values between 0.4 and 2.8, with ~25% of the sets having values >2, and a maximum band per meter ranging from 6 to 67, with ~70% of the sets having values <30. In contrast, normal band sets have cluster factor values between 1.4 and 8.8, with >80% having values >2, and maximum band per meter ranging from 9 to 161, with ~70% having values >30. This synthetic data set analysis shows two different and little-overlapping graphical domains for reverse and normal band sets, revealing that sets formed in the reverse tectonic regime (contraction) are generally more spatially distributed than sets formed in the normal tectonic regime (extension). Large cluster factor values also seem possible for the strike-slip regime. Beyond the fact that the amount of strike-slip data has no significant statistical weight, this low amount of data allows questioning the extent of their occurrence in porous sandstones.

DISCUSSION

The global data set presented in Figure 2 clearly shows that reverse bands are more spatially distributed than normal bands, which are characterized by more clustered distributions. This difference in organization reveals that tectonic regime is a prominent factor for the distribution of deformation bands in porous sandstone. However, the presence of faults and even primary lithologic heterogeneities seem to be factors that can influence the distribution of bands in reverse band sets (Fig. 1E), but do not control the general trend. Spatially distributed band sets have also been observed in extensional settings, but in specific settings such as in relay zones (e.g., Davatzes and Aydin, 2003) or in cases where strong lithological contrasts impede the propagation of SBs (Schultz and Fossen, 2002).

This influence of tectonic context can be explained by the difference in stress paths occurring in sandstone under normal and reverse tectonic regimes (Soliva et al., 2013). Relatively low mean stress inherent to tectonic extension leads to a localized Byerlee-type cataclastic shear behavior, whereas high mean stress promoted by tectonic contraction leads to distributed compactional-cataclastic behavior (for the mechanical explanation, see the Data Repository; for the behavior of porous sandstones, see Wong and Baud, 2012). This analysis therefore suggests that remote tectonic stress has a stronger influence on band distribution in general than local stress, such as provided by reactivation of inherited faults, layering, or fault segmentation.

[1]GSA Data Repository item 2016137, references for Figures 1 and 2, mechanical explanation and capillary pressure method for Figure 3, is available online at www.geosociety.org/pubs/ft2016.htm, or on request from editing@geosociety.org or Documents Secretary, GSA, P.O. Box 9140, Boulder, CO 80301, USA.

Because deformation bands are well known to be subseismic structures, the exposed evidence of different strain localization together with differences in petrophysical properties between shear-dominated and compaction-dominated bands provide important conclusions for the management of sandstone reservoirs. Compilation of recent data shows that permeability is significantly lower in shear-dominated bands compared to compaction-dominated bands (Ballas et al., 2015), but rather than permeability, capillary pressure is an efficient indicator of the ability of a fault to act as a barrier to fluid flow over geologic time. A new compilation of capillary pressure and porosity (Fig. 3), measured both in reverse and normal band sets sampled in the field, clearly shows that the capillary pressure is generally higher for normal bands than for reverse bands (for method of capillarity calculation, see the Data Repository). This implies the presence of seals and stronger permeability anisotropy in porous sandstone reservoirs affected by tectonic extension, as compared to sandstones affected by contraction. Such a basic new rule of tectonic control of fluid flow and compartmentalization in sandstone reservoir is of major importance for both economic fluid exploration and production and CO_2 storage planning.

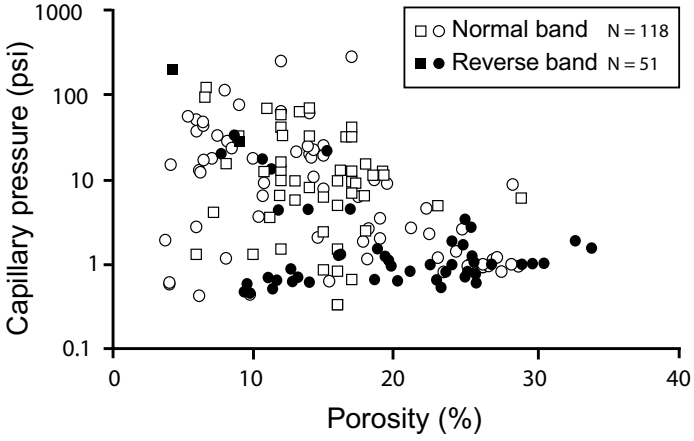

Figure 3. Compiled data for capillary pressure and porosity measured on samples from reverse and normal bands. Squares and circles are for direct and indirect measures, respectively (for method and data references, see the Data Repository [see footnote 1]).

ACKNOWLEDGMENTS

This work was funded by a post-doctoral project at the Laboratory Géosciences Montpellier (University of Montpellier) in collaboration with the University of Bergen. We thank Chia-Yu Lu from the National Taiwan University for his help in the field, editor James Spotila, Stephen Laubach, and two anonymous reviewers for their constructive comments.

REFERENCES CITED

Antonellini, M.A., Aydin, A., and Orr, L., 1999, Outcrop-aided characterization of a faulted hydrocarbon reservoir: Arroyo Grande oil field, California, USA, *in* Haneberg, W.C., et al., eds., Faults and subsurface fluid flow in the shallow crust: American Geophysical Union Geophysical Monograph 113, p. 7–26, doi:10.1029/GM113p0007.

Aydin, A., 1978, Small faults formed as deformation bands in sandstone: Pure and Applied Geophysics, v. 116, p. 913–930, doi:10.1007/BF00876546.

Ballas, G., Soliva, R., Benedicto, A., and Sizun, J.-P., 2014, Control of tectonic setting and large-scale faults on the basin-scale distribution of deformation bands in porous sandstone (Provence, France): Marine and Petroleum Geology, v. 55, p. 142–159, doi:10.1016/j.marpetgeo.2013.12.020.

Ballas, G., Fossen, H., and Soliva, R., 2015, Factors controlling permeability of cataclastic deformation bands and faults in porous sandstone reservoirs: Journal of Structural Geology, v. 76, p. 1–21, doi:10.1016/j.jsg.2015.03.013.

Davatzes, N.C., and Aydin, A., 2003, Overprinting faulting mechanisms in high porosity sandstones of SE Utah: Journal of Structural Geology, v. 25, p. 1795–1813, doi:10.1016/S0191-8141(03)00043-9.

Eichhubl, P., Hooker, J., and Laubach, S.E., 2010, Pure and shear-enhanced compaction bands in Aztec Sandstone: Journal of Structural Geology, v. 32, p. 1873–1886, doi:10.1016/j.jsg.2010.02.004.

Fortin, J., Shubnel, A., and Guégen, Y., 2005, Elastic wave velocities and permeability evolution during compaction of Bleurswiller Sandstone: International Journal of Rock Mechanics and Mining Sciences, v. 42, p. 873–889, doi:10.1016/j.ijrmms.2005.05.002.

Fossen, H., and Bale, A., 2007, Deformation bands and their influence on fluid flow: American Association of Petroleum Geologists Bulletin, v. 91, p. 1685–1700, doi:10.1306/07300706146.

Fossen, H., Schultz, R.A., Shipton, Z.K., and Mair, K., 2007, Deformation bands in sandstone: A review: Journal of the Geological Society [London], v. 164, p. 755–769, doi:10.1144/0016-76492006-036.

Fossen, H., Zuluaga, L.F., Ballas, G., Soliva, R., and Rotevatn, A., 2015, Contractional deformation of porous sandstone: Insights from the Aztec Sandstone in the footwall to the Sevier-age Muddy Mountains thrust, SE Nevada, USA: Journal of Structural Geology, v. 74, p. 172–184, doi:10.1016/j.jsg.2015.02.014.

Klimczak, C., and Schultz, R.A., 2013, Fault damage zone origin of the Teufelsmauer, Subhercynian Cretaceous Basin, Germany: International Journal of Earth Sciences, v. 102, p. 121–138, doi:10.1007/s00531-012-0794-z.

Nicol, A., Childs, C., Walsh, J.J., and Schafer, K.W., 2013, A geometric model for the formation of deformation band clusters: Journal of Structural Geology, v. 55, p. 21–33, doi:10.1016/j.jsg.2013.07.004.

Saillet, E., and Wibberley, C.A.J., 2010, Evolution of cataclastic faulting in high-porosity sandstone, Bassin du Sud-Est, Provence, France: Journal of Structural Geology, v. 32, p. 1590–1608, doi:10.1016/j.jsg.2010.02.007.

Schultz, R.A., and Balasko, C.M., 2003, Growth of deformation bands into echelon and ladder geometries: Geophysical Research Letters, v. 30, p. 2033–2036, doi:10.1029/2003GL018449.

Schultz, R.A., and Fossen, H., 2002, Displacement-length scaling in three dimensions: The importance of aspect ratio and application to deformation bands: Journal of Structural Geology, v. 24, p. 1389–1411, doi:10.1016/S0191-8141(01)00146-8.

Schultz, R.A., Soliva, R., Fossen, H., Okubo, C., and Reeves, D.M., 2008, Dependence of displacement-length scaling relations for fractures and deformation bands on the volumetric changes across them: Journal of Structural Geology, v. 30, p. 1405–1411, doi:10.1016/j.jsg.2008.08.001.

Soliva, R., Schultz, R.A., Ballas, G., Taboada, A., Wibberley, C.A.J., Saillet, E., and Benedicto, A., 2013, A model of strain localization in porous sandstone as a function of tectonic setting, burial and material properties; new insight from Provence (SE France): Journal of Structural Geology, v. 49, p. 50–63, doi:10.1016/j.jsg.2012.11.011.

Solum, J.G., Brandenburg, J.P., Naruk, S.J., Kostenko, O.V., Wilkins, S.J., and Schultz, R.A., 2010, Characterization of deformation bands associated with normal and reverse stress states in the Navajo Sandstone, Utah: American Association of Petroleum Geologists Bulletin, v. 94, p. 1453–1475, doi:10.1306/01051009137.

Wibberley, C.A.J., Petit, J.-P., and Rives, T., 2007, The mechanics of fault distribution and localization in high-porosity sands, Provence, France, *in* Lewis, H., and Couples, G.D., eds., The relationship between damage and localization: Geological Society of London Special Publication 289, p. 19–46, doi:10.1144/SP289.3.

Wong, T.-f., and Baud, P., 2012, The brittle-ductile transition in porous rock: A review: Journal of Structural Geology, v. 44, p. 25–53, doi:10.1016/j.jsg.2012.07.010.

Manuscript received 2 December 2015
Revised manuscript received 6 April 2016
Manuscript accepted 6 April 2016

Printed in USA